

Long-term Change in Summer Water Vapor Transport over South China in Recent Decades

Xiuzhen LI

*Center for Monsoon and Environment Research, Sun Yat-Sen University, Guangzhou, China
Guy Carpenter Asia-Pacific Climate Impact Centre, School of Energy and Environment,
City University of Hong Kong, Hong Kong, China*

Zhiping WEN

Center for Monsoon and Environment Research, Sun Yat-Sen University, Guangzhou, China

and

Wen ZHOU

*Guy Carpenter Asia-Pacific Climate Impact Centre, School of Energy and Environment,
City University of Hong Kong, Hong Kong, China*

(Manuscript received 17 May 2010, in final form 3 November 2010)

Abstract

This article investigated the long-term variation of the boreal summer (JJA) moisture circulation over South China (SC). The total precipitable water (TPW) and moisture convergence over SC have increased obviously, such trend is not a local phenomenon, but the result of large-scale circulation anomaly. In the past few decades, the water vapor transport from southern hemisphere and subtropical western Pacific is strengthened, while the northward transport over East Asia is weakened, leading enhanced moisture convergence over the Philippines and adjacent region. The net flux of SC shows no significant shift in the end of the 1970s which is widely acknowledged as “climate shift”, but ascends remarkably after the early 1990s. This doesn’t mean the moisture circulation over SC experiences no variation with the “climate shift”. In fact, the relationship between total net flux with budgets of four boundaries had been modified in the end of the 1970s. The correlation of the net flux is highly negative with the budget of north boundary, and positive with the budget of west and east boundaries before 1979/80, but only highly positive with the budget of south boundary after 1979/80.

This modification is closely related to the north-south migration of western Pacific subtropical high (WPSH). Before 1979/80, the ridge of WPSH lies northward, resulting in stronger output of water vapor via the north boundary which may probably lead to the significant correlation between flux of north boundary and net flux. After 1979/80, the ridge of WPSH shifts southward, inducing stronger water vapor input through the south boundary, which is probably the causation of significant correlation between flux of south boundary and net flux.

1. Introduction

Water vapor transported by the atmospheric circulation is one of the most important processes in water cycle; water vapor transported from outside and its convergence are closely related to the amount of regional precipitation. Only an average layer of 25 mm deep over the entire globe can be

Corresponding author: Wen Zhou, Guy Carpenter Asia-Pacific Climate Impact Centre, School of Energy and Environment, City University of Hong Kong, Hong Kong, China.
E-mail: wenzhou@cityu.edu.hk
© 2011, Meteorological Society of Japan

created if all water vapor in atmosphere is precipitated (UNESCO 1978). Zhou and Yu (2005) emphasized the importance of water vapor transport in the East Asian monsoon system, and pointed out that the anomalous water vapor supply could directly lead to extreme drought/flood. In recent decades, as pointed out by the 2007 report of Intergovernmental Panel on Climate Change (IPCC) that the surface humidity has gone up after 1976, the total column water vapor over global oceans has increased by $1.2 \pm 0.3\%$ per decade from 1988 to 2004, and there is also dramatic change in large scale circulation such as ENSO and Asia monsoon (Trenberth et al. 2007; Wang et al. 2007, 2009).

Huang et al. (1998) found that the water vapor convergence over East Asia is mainly due to the water vapor advection caused by monsoonal flow. The contributions of the moisture transport from the tropical oceans, such as the Northern Indian Ocean, the South China Sea (SCS) and the western Pacific Ocean are vital for rainfall pattern in China (Simmond et al. 1999; Ninomiya and Kobayashi 1999; Ding and Sun 2001). Further, the water vapor transport over China is also affected by the mid-latitude circulation and the western Pacific subtropical high (Lau and Li 1984; Tao and Chen 1987; Nan and Li 2003). Zhou and Yu (2005) pointed out that the anomalous water vapor transport related to typical anomalous rainfall anomalies in China might be associated with a southward extension of the western Pacific subtropical high. However, the water vapor transports in association with these changes are not well addressed.

South China is located in the southeast part of Asia, bordered by the northwestern Pacific, and influenced by a typical monsoon circulation. In summer, a large amount of moisture is carried into South China from the adjacent ocean via monsoonal circulation and contributes to the precipitation over South China. Numerous studies reveal that rainfall over South China is experiencing dramatic long-term change in the past few decades (Nitta and Hu 1996; Weng et al. 1999; Gong and Wang 2000; Chan and Zhou 2005; Zhou et al. 2005, 2006; Wang et al. 2006; Yuan et al. 2008a,b). The mean rainfall over South China in the 1990s is higher than for any other decades, which is unprecedented in the record since 1880 (Gong and Wang 2000). Not only the total amount of precipitation, but also the frequency of extreme rainfall events over South China increased in recent decades (Zhai et al. 2005).

Former studies on moisture circulation focused mainly on either normal conditions or particular cases (Tao and Chen 1987; Huang et al. 1998; Simmond et al. 1999; Zhou et al. 2009); the long-term change of water vapor transport over South China has seldom been investigated. Does the moisture budget over South China experience dramatic change in recent decades? And, what possible mechanism is responsible for this change? To solve these questions, the long-term variation of the water vapor transport over South China is investigated. In this study, data and methodology are introduced in Section 2. The climatological characteristic, long-term change of vertically integrated water vapor transport and regional moisture budget of South China will be investigated in Section 3. Finally, summary and discussion will be included in Section 4.

2. Data and methodology

2.1 Data

Global reanalysis dataset provided by European Centre for Medium-Range Forecasts (ECMWF) 40 Years Re-Analysis (ERA-40) in boreal summer (June–August; JJA) for the period of 1958–2002 are used to estimate the vertically integrated water vapor flux. The physical variables used in this study include the four-time daily specific humidity, meridional, zonal wind components and so on. Since virtually most of the water vapor in the atmosphere occurs below 200 hPa, only analyses for the surface and eleven lowest mandatory levels (1,000, 925, 850, 775, 700, 600, 500, 400, 300, 250, 200 hPa) are included in the calculation. The monthly geopotential height at 500 hPa is also used to describe the circulation pattern. The horizontal resolution is $2.5^\circ \times 2.5^\circ$ latitude-longitude (Uppala et al. 2005).

For the purpose of revealing the relationship between precipitation and water vapor flux, the observed precipitation data from 730 stations in China has been used to analyze the amount of summer rainfall in South China. Figure 1 shows the climatic mean summer precipitation over most of China. The values in excess of 400 mm are located on South China, to the south of 32.5°N . Considering the precipitation to the west of 105°E is mainly induced by the orographic dynamic lifting which differs from that to the east, we focus primarily on the region to the east of 105°E in this study.

2.2 Atmospheric water vapor balance

The general balance equation for atmospheric water vapor, if the flux across the upper boundary,

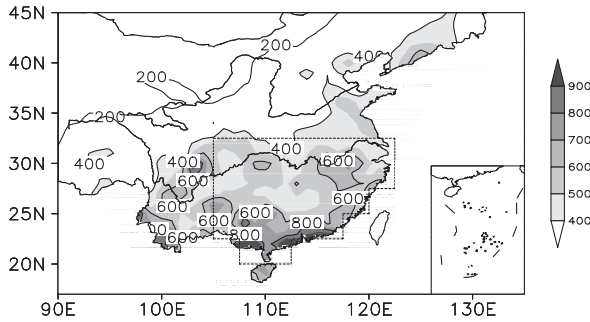


Fig. 1. Spatial distribution of climatic mean summer (JJA) precipitation for the period of 1958–2002 over China (unit: mm season⁻¹). Only values that over 400 are shaded. The dashed polygon indicates the target region which is defined as South China in this study.

diffusion, liquid and solid phase transport are neglected, can be expressed as (Schmitz and Mullen 1996):

$$\partial W / \partial t = -\nabla \cdot \vec{Q} + E - P. \quad (1)$$

Here, E and P are evaporation and precipitation respectively; W is the total precipitable water, defined by

$$W = \frac{1}{g} \int_{p_t}^{p_s} q dp, \quad (2)$$

and \vec{Q} is the vertically integrated water vapor flux:

$$\vec{Q} = \frac{1}{g} \int_{p_t}^{p_s} q \vec{V} dp. \quad (3)$$

Where g is the acceleration of gravity, q is specific humidity, \vec{V} is the horizontal wind vector, p_s is the surface pressure, and p_t is the pressure at the top of the atmosphere, which is set as 200 hPa in this study. Since q and p_s are lacking in the surface variables list of ERA-40, those are calculated from other variables, including the sea level pressure, surface temperature, dew point temperature and geopotential height.

Water vapor flux can be partitioned into stationary and transient eddy components according to conventional breakdown:

$$\overline{q\mathbf{u}} = \overline{q\mathbf{u}} + \overline{q'\mathbf{u}'}. \quad (4)$$

The stationary component is calculated by using monthly mean data while the transient eddy component is evaluated as the departures from individual monthly mean values by using four-time daily data (Zhou and Yu 2005).

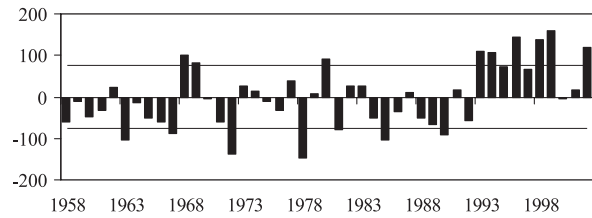


Fig. 2. Time series of the regional summer (JJA) precipitation anomalies over South China from 1958 to 2002 (unit: mm season⁻¹). The horizontal lines represent the associated one time standard deviation ($\pm 1\sigma$).

3. Results

3.1 Vertically integrated water vapor flux

The observed precipitation data is employed to estimate the interannual summer precipitation over South China. The 45-yr mean of the summer rainfall over South China is 587 mm. Figure 2 shows the time series of the regional summer rainfall anomalies over South China. South China is the region shown as the dashed polygon in Fig. 1, with the western boundary lying on 105°E, northern boundary on 32.5°N; the eastern and southern boundary are defined based on the land-ocean edge, the eastern boundary is located near 120°E, the southern boundary is located near 22.5°N. The standard deviation (σ) of summer rainfall over 1958–2002 is 76 mm. The “wet” years defined here are the years with anomalous rainfall over 1.0σ , that is, 1968, 1980, 1993, 1994, 1995, 1996, 1998, 1999, 2002; the “dry” years are the years 1963, 1967, 1972, 1978, 1985, 1989, 1990, with the anomalous rainfall less than -1.0σ . It is worth noting that there is a significant interdecadal variability in the extreme events; most of the “wet” years happen in the 1990s, while most of the “dry” years happen before the 1990s. This is associated with the abrupt change of summer rainfall around 1992/93 in South China as shown in Fig. 2. The regional rainfall is only 559 mm during 1958–92, while it is significantly increased to 683 mm after 1993. This interdecadal change in summer rainfall over South China was also pointed out by Qian and Qin (2008), Yao et al. (2008) and Wu et al. (2010).

The total precipitable water (TPW) over East Asia is displayed in Fig. 3. South China is located in the vast area of high TPW (>40 mm). The average TPW over South China is over 50 mm,

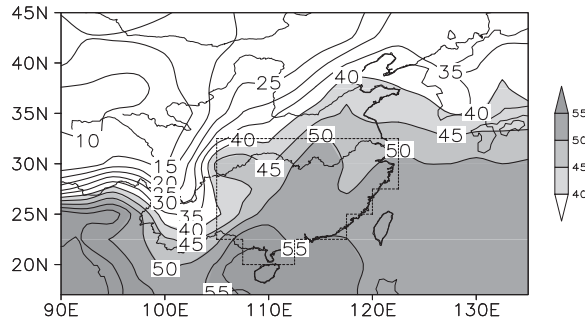


Fig. 3. Spatial distribution of climatic mean summer (JJA) total precipitable water for the period of 1958–2002 over East Asia (unit: mm). Only values over 40 are shaded.

comparable to that over adjacent Pacific Ocean. The spatial distribution of TPW exhibits a light southeast-northwest gradient, with the amounts in excess of 55 mm in the former area and less than 40 mm in the latter. The TPW over South China is much higher than that over other non-monsoon

land regions at the same latitude (figure not shown), which indicates the summer monsoon over South China makes it one of the distinctive humid areas attracting a mass of attentions.

Before going on to discuss the changes in water vapor transport in recent decades, it is important to have an overview of the climatological characteristic of the summer moisture circulation. Figure 4a shows the distribution of climatic mean summer vertically integrated water vapor flux and its divergence from 1958 to 2002. South China is mainly influenced by three branches of water vapor transport from lower latitude: the first is the cross-equator flow around 105°E, which is associated with the strong anticyclonic circulation over Australia; the second is from the tropical Pacific Ocean transported by southerly flow to the west of the WPSH, bringing abundant warm and moist air into South China; the third is transported by the southwest flow of Indian summer monsoon across the Arabian Sea, Bay of Bengal, partitioning into two branches when reaches Indochina Peninsula. One crosses the northern part of Indochina Peninsula

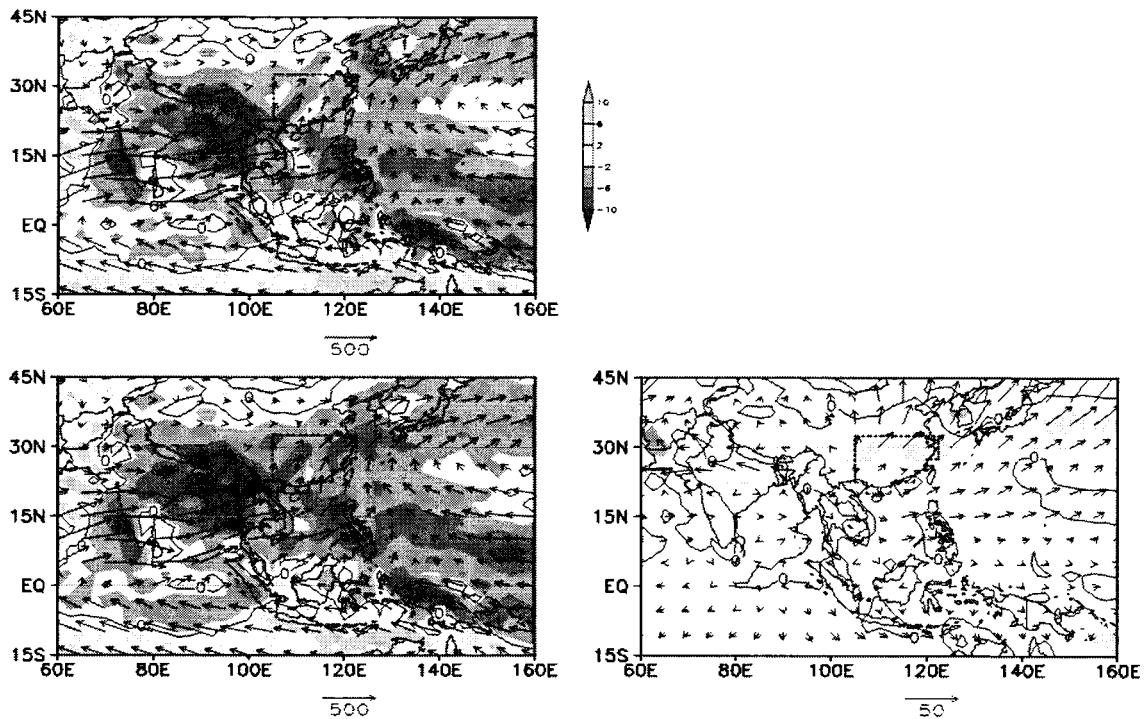


Fig. 4. Time-averaged (1958–2002) summer vertically integrated water vapor transport (vector, unit: $\text{kg m}^{-1} \text{s}^{-1}$) and its divergence pattern (contour and shading, unit: $10^{-5} \text{ kg m}^{-2} \text{ s}^{-1}$). (a) total term, (b) stationary component, (c) transient eddy component. The dark shading represents water vapor convergence, while light shading represents water vapor divergence.

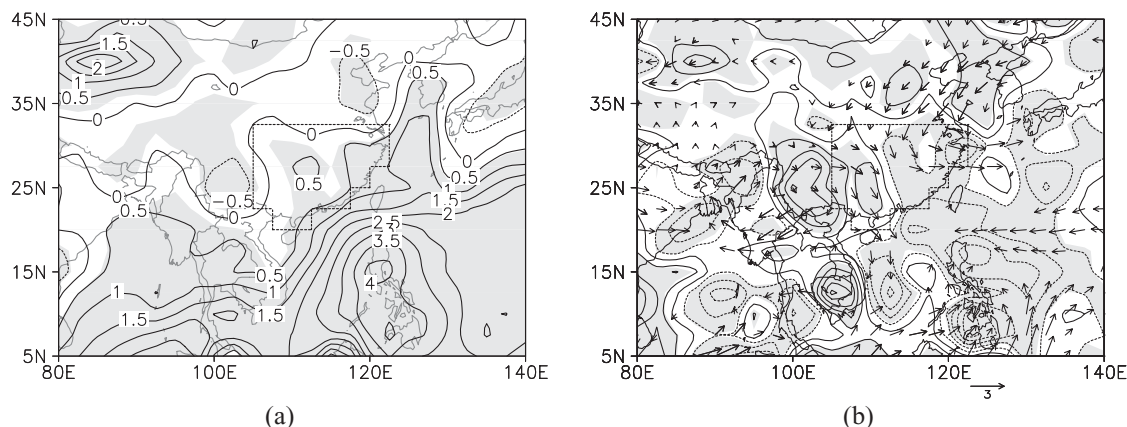


Fig. 5. Distribution of linear tendency for (a) total precipitable water (unit: $\text{mm } 10 \text{ yrs}^{-1}$), (b) water vapor flux (vector, only those over 80% confidence level are shown, unit: $\text{kg m}^{-2} \text{ s}^{-2} 10 \text{ yrs}^{-1}$) and its divergence (contour, unit: $10^{-5} \text{ kg m}^{-2} \text{ s}^{-1} 10 \text{ yrs}^{-1}$). Shading in (a), (b) denotes regions where the tendency is significant at the 90% confidence level according the Student-t test. Contour interval in (b) is $0.5 \times 10^{-5} \text{ kg m}^{-2} \text{ s}^{-1} 10 \text{ yrs}^{-1}$.

and transports northeastward to the western boundary of South China on the middle troposphere, the other transports eastward, converges with two flows mentioned above over SCS, turns northward and transports to South China. The corresponding time-averaged summer water vapor divergence pattern is also shown in Fig. 4a as shaded. Sink regions are situated over the wide area of South Asia, East Asia and western Pacific Ocean which are influent by the southwest and southeast monsoons. The convergence center is located on the west coast of the Indian Peninsula and the Philippines, and the southern slope of Tibetan Plateau which is consistent with the summer rainfall pattern (not shown). South China is subject to the water vapor convergence as expected.

The roles played by the stationary and transient eddy components of the flux respectively are also of our interest in this study. Broken down total water vapor flux into stationary and transient eddy components (Figs. 4b, c), it can be found that the stationary component is comparable to the total flux not only in magnitude but also in spatial distribution. The transient eddy component trends to assume its largest value at mid-high latitude, transporting water vapor out of South China to the northeast. However, it's almost one order less than the total flux in magnitude. Analyzing the divergence of stationary and eddy water vapor flux, not unexpectedly, Fig. 4b strongly resembles Fig. 4a that South China is located within the vast convergent area. The eddy component is mainly responsi-

ble for the weak divergence, with the largest value center lying over the Yangtze River Basin, on the north of South China. Generally speaking, the water vapor transport over South China is mostly dominated by the stationary component; the eddy component is so small that can be neglected. This coincides with the conclusions of Zhou et al. (1999) and Simmonds et al. (1999).

Consistent with the long-term change of precipitation over South China as mentioned above, the TPW over South China increases dramatically, contrasting to decreasing trend to the north and the west of South China (Fig. 5a). In fact, a vast tropical regions over eastern Indian Ocean, western Pacific, eastern Pacific and western Atlantic Ocean experience an obvious increase in TPW, with the maximum linear tendency ($>3.5 \text{ mm } 10 \text{ yrs}^{-1}$) over Philippine, to the southeast of South China. The distribution of linear tendency over water vapor flux convergence displays a similar pattern. The water vapor convergence of North and West China weakens, while the convergence over most part of South China strengthens. A strong anomalous convergent center is located over Philippine and South China is situated at its northwest part (Fig. 5b). The tendency of water vapor convergence is closely associated with the change of water vapor flux. From 1958 to 2002, the water vapor transport to western Pacific from southern hemisphere to the east of 120°E and from subtropical western Pacific strengthen, while the northward transport to the north of East Asia decreases; these three anomalous

Table 1. Total water vapor transport across the four boundaries, the corresponding regional water vapor budgets (unit: mm, after dividing by the area of the target domain) and regional averaged flux divergence ($\text{kg m}^{-2} \text{s}^{-1}$) over South China. Positive (negative) values denote inflow (outflow) through each boundary or regional net gain (loss) of water vapor.

Layer (hPa)	Southeast China					
	W*	E*	S*	N*	Net*	Div*
400–200	22	–30	1	–8	–14	1.5×10^{-6}
775–400	187	–348	451	–281	8	-2.7×10^{-6}
sfc-775	–7	–168	797	–325	297	-33.4×10^{-6}
sfc-200	202	–546	1250	–615	291	-34.6×10^{-6}

*W = western boundary; E = eastern boundary; S = southern boundary; N = northern boundary; four boundaries of South China is shown in dashed line in Fig. 1; Net = net flux; Div = regional average divergence.

water vapor paths result in strong water vapor convergence over vast region over Philippine and SCS with South China at its northwest part. It indicates that the wetter trend over South China is not just a local phenomenon, but connected to the large-scale circulation regime shift.

3.2 Moisture budget

a. Regional atmospheric moisture budget

To have a look at the amount of regional moisture budget and flux divergence, fluxes via four boundaries and their vertical structure, regional moisture budget, flux divergences and fluxes across the regional boundaries are calculated for the low (surface to 775 hPa), middle (775–400 hPa), high (400–200 hPa) layers and total column (surface to 200 hPa) over South China (Table 1). The layers are divided considering the consistency of moisture circulation structure of levels in each layer, which are also agree with the study of Simmonds et al. (1999). Western and southern boundaries are the input boundaries; Total column water vapor flux of the latter (1,250 mm) is much larger than, nearly six times of the former (202 mm), which indicates only nearly 14% water vapor input originates from Bay of Bengal by the way of northern Indochina Peninsula, while 86% water vapor is transported into South China Through SCS, which is a key region for the summer moisture transport over South China. Eastern and northern boundaries are the output boundaries with the magnitudes of two (546 mm and 615 mm) are comparable. The net

moisture budget of South China is the results from the four boundaries combined. It is the small values calculated from several large values. Studying more details about vertical distribution of water vapor budget, we can find that the water vapor inflow of the western boundary lies mainly in the middle layer, with water vapor budget of the low layer negative. The outflow of eastern boundary also lies mainly in the middle level, about twice as that of the low layer, ten times larger than that of the high layer. Different from the western boundary, the inflow via southern boundary is mainly in the low layer, about 1.77 times as that in the middle layer. The outflows via northern boundary in the low and middle layer are comparable. The net gain of water vapor in the low layer is principal, much higher than that of middle layer, while that of the high layer is negative, denoting that the water vapor is mainly convergent in the low layer, divergent in the high layer; it is consistent with the vertical distribution of regional average water vapor flux divergence.

b. Variability of atmospheric moisture budget

Time series of the water vapor fluxes across four regional boundaries and net gain of water vapor of South China (Fig. 6) reveal that: (1) the interannual variations of water vapor flux of the eastern and western boundaries are remarkable and similar (the correlation between total flux of eastern and western boundaries is 0.86); the stationary components are much larger than the eddy components, which indicates that the zonal water vapor transport of South China is controlled by similar large-scale circulation. (2) Interannual variations of water vapor flux of the southern and northern boundaries are dissimilar; the stationary component is much larger than the eddy component in the southern boundary, while slightly larger than eddy component in the northern boundary. (3) The linear tendencies of moisture budgets are increasing in the eastern and western boundaries while descending in northern boundary. The linear tendency of southern boundary is slightly descending before 1979/80, while ascending after 1979/80. These linear tendencies are significant over the 80% confidence level. (4) The time series of net flux is similar to that of the precipitation over South China (Fig. 2), with correlation coefficient between them over 0.82, which is significant at the 99% confidence level. It is worth mentioning that the net flux of South China does not show significant shift in the end of the 1970s when enhanced global warming

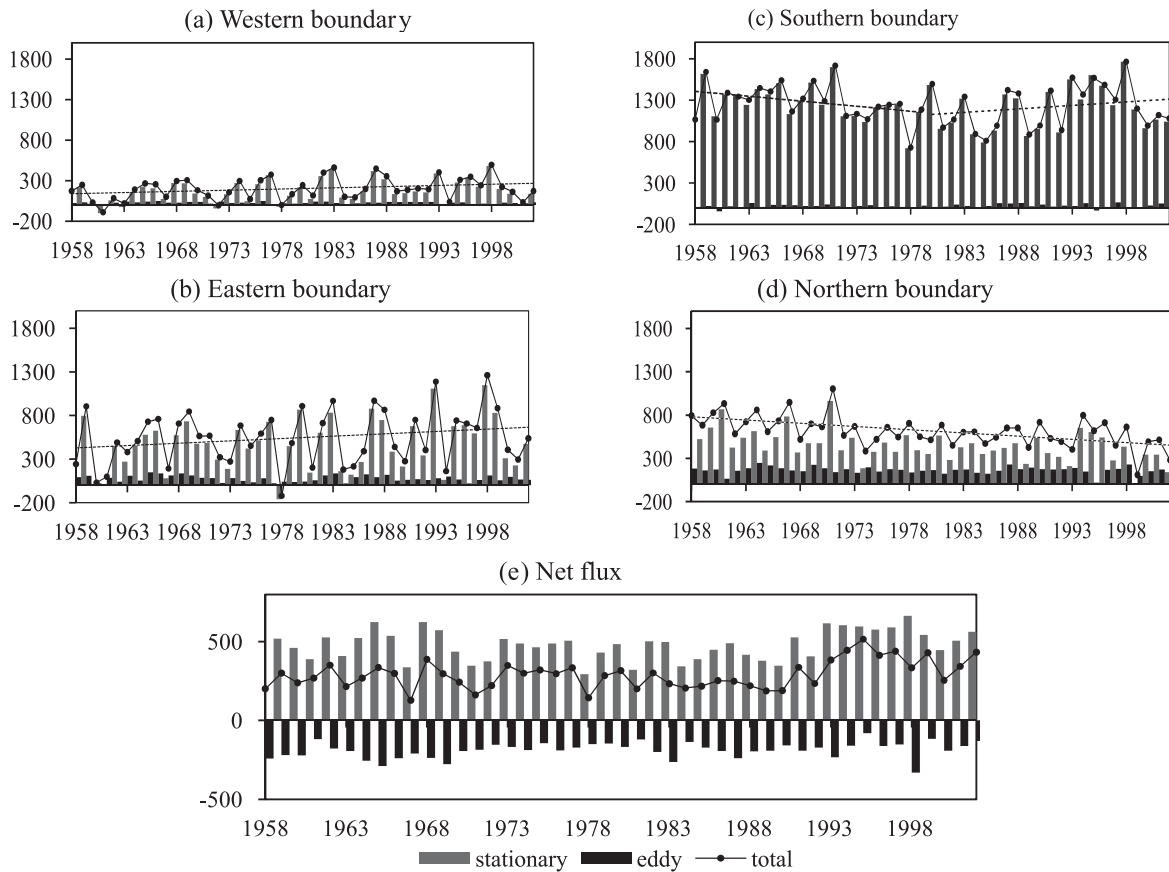


Fig. 6. Time series of fluxes across four regional boundaries and net flux of South China (unit: mm). (a) western boundary, (b) eastern boundary, (c) southern boundary, (d) northern boundary, (e) net flux. The positive value is defined as eastward flux in the zonal direction, northward flux in the meridional direction. The gray bars indicate stationary component, the black bars indicate transient eddy component, the solid curves indicate total water vapor flux, and the dashed lines indicate the tendency of the fluxes. The western boundary defined here is on 105°E , northern boundary is on 32.5°N , the eastern and southern boundary are defined based on the land-ocean edge, that is, the eastern boundary is located near 120°E , the southern boundary is located near 22.5°N as shown in Fig. 1.

emerged, but shows remarkable ascending in the early 1990s, which is significant at the 95% confidence level according to the Mann-Kendall test (Mann 1945; Kendall 1955). Is it indicating that whether there is any relationship between the water vapor budget of South China and the ‘climatic shift’ in the mid 1970s? Actually, the answer is negative, it will be analyzed below.

To illustrate which boundary influence the net flux of South China most seriously, and if that boundary vary in the past few decades, the 19 years’ running correlation between total term, stationary component, eddy component of budget for each boundary and total term budget of South

China is shown in Fig. 7. The correlation of total-term budget of South China with budget of each boundary in total term is similar to that in stationary term, while comparatively small and insignificant in eddy term. Total-term budget of South China is mainly relative to the stationary-component but not to the eddy-component budget of each boundary. Thus, the study below is mainly based on the stationary component. It is also worthy to be noted that the running correlations of net flux with budget of east and west boundary are similar, which are high before the middle of the 1970s, but decrease with time; the phases of running correlations of net flux with budget of south and north

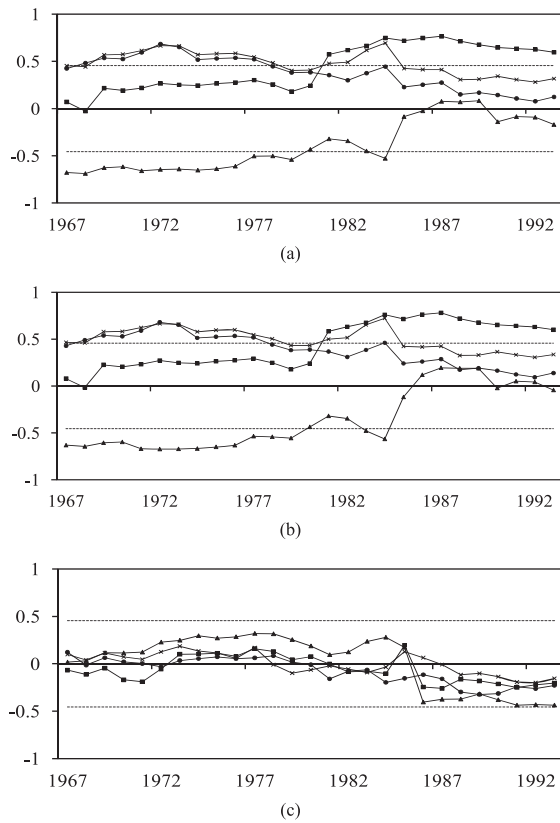


Fig. 7. 19 years' running correlations between (a) total flux, (b) stationary component, (c) transient eddy component of each boundary and total net flux of South China. Lines with solid circle represent the western boundary, line with forks represent the eastern boundary, lines with solid squares represent the southern boundary, line with solid triangles represent the northern boundary. The gray dashed lines represent the 95% confidence level according to the Student-t test.

boundary are opposite (Fig. 7b). The net flux of South China's correlation is highly negative before 1979/80, but insignificant after 1979/80 with the budget of north boundary; however, it is insignificant before 1979/80, but highly positive after 1979/80 with the budget of south boundary. Thus, the correlations between total net flux with fluxes of four boundaries had changed in the end of the 1970s.

4. Summary and discussion

In this study, long-term variation of the water vapor transport over South China in the past

decades is investigated using the ECMWF ERA-40 dataset for the period of 1958–2002. It is found that South China is one of the distinctive humid areas, with the average TPW over 50 mm, much higher than that over other non-monsoon regions on the same latitude. South China is located in vast water vapor convergent area over South Asia and Western Pacific, mainly influenced by three branches of water vapor transport from lower latitude. The total water vapor flux includes stationary and transient eddy components, with the former comparable to, while the latter almost one order less than the total flux. In other words, water vapor transport over South China is mostly dominated by the stationary component, and the eddy component can be neglected. In the past few decades, the TPW over South China increased obviously. And, the water vapor transport from southern hemisphere and subtropical western Pacific Ocean increased, while the northward transport over east China decreased; these three anomalous water vapor paths result in stronger water vapor convergence over northwestern Pacific Ocean and our target domain. The wetter trend over South China is the result of large-scale circulation anomaly, not just a local phenomenon.

The moisture budgets are increasing in the eastern and western boundaries while descending in northern boundary. The budget of southern boundary is slightly descending before 1980, while ascending after 1980. The net flux does not show significant shift in the end of the 1970s which is widely acknowledged as “climate shift”, but ascends remarkably by the early 1990s.

The running correlations of net flux with budget of eastern and western boundaries are similar, which are high before the mid the 1970s, but decrease with time; the running correlation of net flux is highly negative before 1979/80, but insignificant after 1979/80 with the budget of northern boundary, while insignificant before 1979/80, but highly positive after 1979/80 with the budget of southern boundary. Thus, the correlations between total net flux with budgets of four boundaries had been changed in the end of the 1970s.

Our results support that there is a shift in the relationship of total flux and budgets of four boundaries in the end of the 1970s. But, what is the main factor resulting in this shift? Why does this shift take place in the end of the 1970s? Before making an explanation, circulation that closely associated with the fluxes of four boundaries should be found

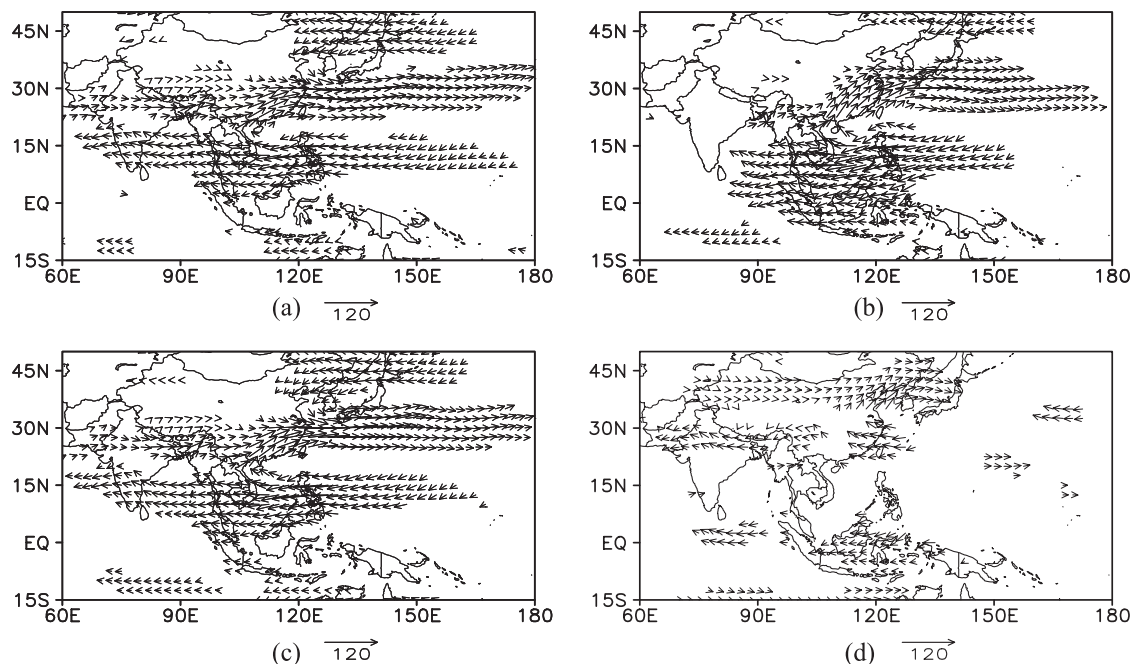


Fig. 8. Regressions of anomalous summer vertically integrated water vapor flux upon fluxes of four boundaries (unit: kg/m/s). (a) western boundary, (b) southern boundary, (c) eastern boundary, (d) northern boundary. Only values that significant over 99% confidence level according the Student-t test are shown.

out. Regressions of anomalous summer vertically integrated water vapor flux upon budgets of four boundaries (Fig. 8) show that the regressed water vapor circulation upon budgets of western, eastern boundaries are similar. That is the anticyclonic circulation of the WPSH lying in the mid-low latitude, the westerlies anomalies to the west of South China and the cyclonic circulation anomalies to the north of South China. It implies that the west and east boundaries are under the control of similar atmospheric circulation, which has been concluded before. However, there are great differences in the regressed fields based on the budget of the southern and northern boundaries. The budget of southern boundary is closely related to the intensity of the anticyclonic water vapor transport to the west of WPSH in low latitude. When the WPSH drifts southward, the anticyclonic water vapor transport to the west of WPSH strengthens, resulting in more water vapor transported into South China via southern boundary. Contrarily, the budget of north boundary is mainly relative to the intensity of anticyclonic water vapor transport located in the mid-high latitude. Hence, the intensity of fluxes of south and north boundaries is highly influent by

the position of WPSH. The north-south migration of WPSH can seriously affect the water vapor flux over South China.

Some researches show that there is a pronounced decadal variation of the activity of WPSH in the end of 1970s (Yang et al. 2006; Gong and Ho 2002). Referring to Peng (2000), the ridge index of WPSH is defined as the average latitude in which the geopotential height at 500 hPa is largest ($H_{\max} \geq 5,865$ gpm) between the latitude of 15°N to 45°N on the domain of 110°–150°E. The long-term mean position of the ridge of WPSH in summer is located near 25°N. Time series of ridge index of WPSH deviation (Fig. 9) reveal that the ridge index of WPSH anomaly varies within $\pm 4^\circ$ N, the ridge of WPSH lies northward before the end of 1970s while southward after 1980, except for some abnormal years.

How does the northward or southward location of WPSH influence the water vapor transport over South China? Relationship between ridge index of WPSH and water vapor flux before and after 1979/80 in summer (Fig. 10) reveal that the negative correlation between the ridge index and zonal water vapor flux over South China does not experi-

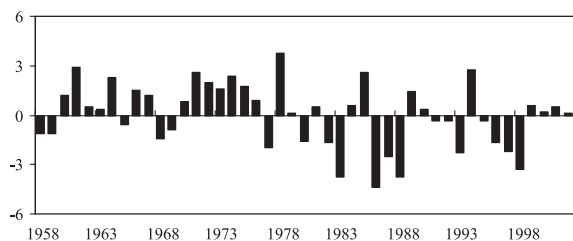


Fig. 9. Time series of ridge index of western Pacific subtropical high (WPSH) anomalies on summer during 1958–2002 (unit: degree). The climatic mean is calculated from the average of 1958–2002.

ence much change before and after 1979/80. That is, when the WPSH shifts southward, the eastward transport over South China increases, and vice versa. However, the relationship between ridge index and meridional water vapor flux over South China changed a lot. The highly significant positive value is located on the north of South China with low negative value on the south before 1979/80.

That is, before 1979/80, when the ridge of WPSH lies northward as described above, it mainly influences the flux of the north boundary, resulting in increasing output of water vapor from South China through north boundary. This mechanism may probably lead to the significant correlation between flux of north boundary and net flux of South China before 1979/80 (Fig. 7). Instead, after 1979/80, the high significant value lies in the south of South China with low positive value in the north. That is, after 1979/80, the ridge of WPSH lies southward, inducing increasing water vapor input via south boundary, resulting in increasing net flux into South China, which is probably the causation of significant correlation between flux of south boundary and net flux of South China after 1979/80.

It can be concluded that associated with the shift of the ridge of WPSH in the end of the 1970s, the moisture circulation and budgets of four boundaries of South China experience a distinct change, even though the main controlling boundary of South China, has been changed from the northern boundary to the southern boundary. Though the

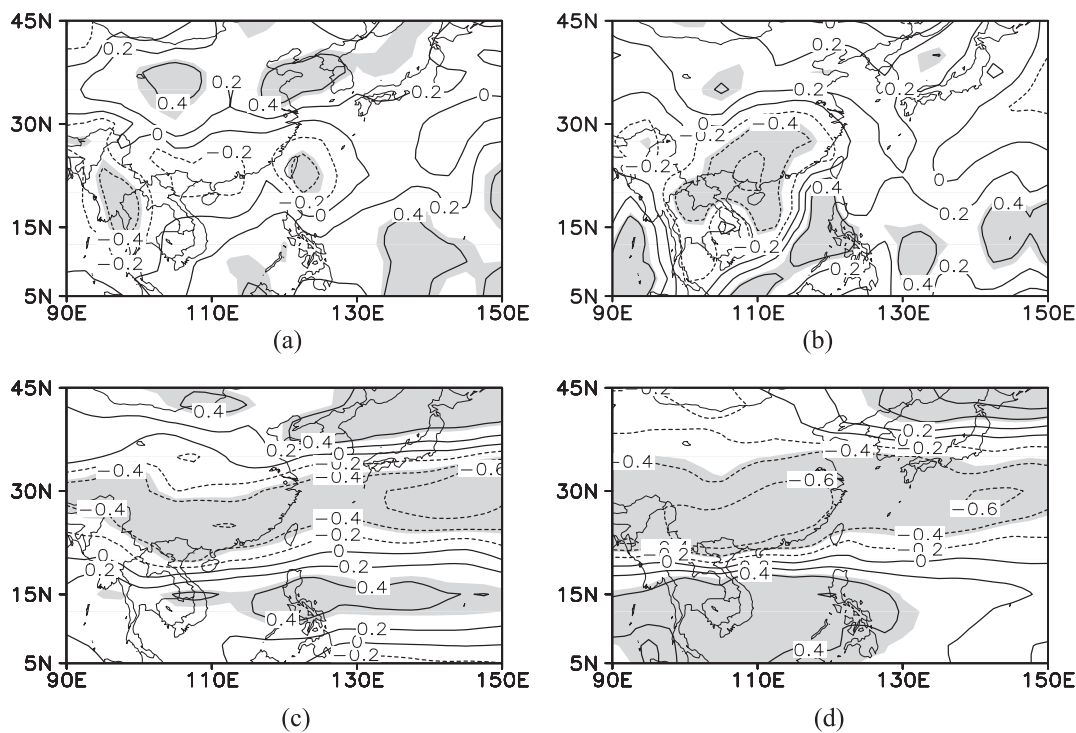


Fig. 10. Correlations between ridge index of WPSH in summer and meridional water vapor flux (a, b), zonal water vapor flux (c, d) for the period of 1958–79 (a, c), 1980–2002 (b, d). The contour interval is 0.2, shading denotes regions where the correlation is significant at the 90% confidence level according to the Student-t test.

budgets of four boundaries of South China undergo significant change in the end of the 1970s, the net flux that closely related to the regional precipitation is decided by the combined action of four boundaries. It is the small value calculated from subtraction of budgets of four boundaries which is much larger. Hence, whereas the moisture circulation over South China has been modified with the “climate shift”, the net water vapor input over South China does not exhibit significant change in that time, but shows abrupt shift in the early 1990s when the stronger convergent circulation take place which still need more attention in further study.

Acknowledgements

The authors would like to thank Dr. Renguang Wu and Dr. Song Yang for their valuable comments and suggestions. This research is sponsored by 973 Basic Research Program Grant (2009CB421401 and 2009CB421404), National Nature Science foundation of China (Grant No. 40730951) and partly supported by the City University of Hong Kong Strategic Research Grants (7002505).

References

- Chan, J. C. L., and W. Zhou, 2005: PDO, ENSO and the summer monsoon rainfall over South China. *Geophys. Res. Lett.*, **32**, L08810.
- Ding, Y. H., and Y. Sun, 2001: A study on anomalous activities of East Asian summer monsoon during 1999. *J. Meteor. Soc. Japan*, **79**, 1119–1137.
- Gong, D. Y., and C. H. Ho, 2002: Shift in the summer rainfall over the Yangtze River valley in the late 1970s. *Geophys. Res. Lett.*, **29**, 1436, doi: 10.1029/2001GL014523.
- Gong, D. Y., and S. W. Wang, 2000: Severe rainfall in China associated with the enhanced global warming. *Climate. Res.*, **16**, 51–59.
- Huang, R. H., Z. Z. Zhang, G. Huang, and B. H. Ren, 1998: Characteristics of the water vapor transport in East Asian monsoon region and its difference from that in South Asian monsoon region in summer. *Scientia Atmospherica Sinica*, **22**, 460–469.
- Kendall, M. G., 1955: *Rank Correlation Methods*, Griffin, London.
- Mann, H. B., 1945: Nonparametric tests against trend, *Econometrica*, **13**, 245–259.
- Nan, S. L., and J. P. Li, 2003: The relationship between the summer precipitation in the Yangtze River valley and the boreal spring Southern Hemisphere annular mode. *Geophys. Res. Lett.*, **30**, 2266, doi: 10.1029/2003GL018381.
- Ninomiya, K., and C. Kobayashi, 1999: Precipitation and moisture balance of the Asian summer monsoon in 1991 part II: Moisture transport and moisture balance. *J. Meteor. Soc. Japan*, **77**, 77–99.
- Nitta, T., and Z. Z. Hu, 1996: Summer climate variability in China and its association with 500 hPa height and tropical convection. *J. Meteor. Soc. Japan*, **74**, 425–445.
- Peng, J. Y., and Z. B. Sun, 2000: Influence of spring equatorial eastern Pacific SSTA on western Pacific subtropical high. *Journal of Nanjing Institute of Meteorology*, **23**, 191–195 (in Chinese).
- Qian, W. H., and A. Qin, 2008: Precipitation division and climate shift in China from 1960 to 2000. *Theor. Appl. Climatol.*, **93**, 1–17.
- Schmitz, J. T., and S. L. Mullen, 1996: Water vapor transport associated with the summertime North American monsoon as depicted by ECMWF analyses. *J. Climate*, **9**, 1621–1634.
- Simmonds, I., D. H. Bi, and P. Hope, 1999: Atmospheric water vapor flux and its association with rainfall over China in summer. *J. Climate*, **12**, 1353–1367.
- Tao, S. Y., and L. X. Chen, 1987: A review of recent research on the East Asian summer monsoon in China. Chang, C. P. and T. N. Krishnamurti (eds.), *Monsoon Meteorology*, Oxford University Press, 60–92.
- Trenberth, K. E., P. D. Jones, P. Ambenje, R. Bojariu, D. Easterling, A. K. Tank, D. Parker, F. Rahimzadeh, J. A. Renwick, M. Rusticucci, B. Soden, and P. Zhai, 2007: Observations: Surface and Atmospheric Climate Change. Solomon S., D. Qin, M. Manning, Z. Chen, M. Marquis, K. B. Averyt, M. Tignor, and H. L. Miller (eds.), *Climate Change 2007: The Physical Science Basis. Contribution of Working Group I to the Fourth Assessment Report of the Intergovernmental Panel on Climate Change*. Cambridge University Press.
- UNESCO, 1978: *World Water Balance and Water Resources of the Earth*, UNESCO Press, 87, 93–99, 587.
- Uppala, S. M., P. W. Kållberg, A. J. Simmons, U. Andrae, V. Da Costa Bechtold, M. Fiorino, J. K. Gibson, J. Haseler, A. Hernandez, G. A. Kelly, X. Li, K. Onogi, S. Saarinen, N. Sokka, R. P. Allan, E. Andersson, K. Arpe, M. A. Balmaseda, A. C. M. Beljaars, L. Van De Berg, J. Bidlot, N. Bornmann, S. Caires, F. Chevallier, A. Dethof, M. Dragosavac, M. Fisher, M. Fuentes, S. Hagemann, E. Hólm, B. J. Hoskins, L. Isaksen, P. A. E. M. Janssen, R. Jenne, A. P. McNally, J. F. Mahfouf, J. J. Morcrette, N. A. Rayner, R. W. Saunders, P. Simon, A. Sterl, K. E. Trenberth, A. Untch, D. Vasiljevic, P. Viterbo, and J. Woollen, 2005: The ERA-40 re-analysis. *Quart. J. Roy. Meteor. Soc.*, **131**, 2961–3012.
- Wang, X., C. Y. Li, and W. Zhou, 2006: Interdecadal variation of the relationship between Indian rain-

- fall and SSTA modes in the Indian Ocean. *Int. J. Climatol.*, **26**, 595–606.
- Wang, X., C. Y. Li, and W. Zhou, 2007: Interdecadal mode and its propagating characteristics of SSTA in the South Pacific. *Meteor. Atmos. Phys.*, **98**, 115–124, DOI:10.1007/s00703-006-0235-2.
- Wang, X., D. Wang, and W. Zhou, 2009: Decadal variability of Twentieth-century El Niño and La Niña occurrence from observations and IPCC AR4 coupled models. *Geophys. Res. Lett.*, **36**, L11701, doi:10.1029/2009GL037929.
- Weng, H. Y., K. M. Lau, and Y. K. Xue, 1999: Multi-scale summer rainfall variability over China and its long-term link to global sea surface temperature variability. *J. Meteor. Soc. Japan*, **77**, 845–857.
- Wu, R. G., Z. P. Wen, S. Yang, and Y. Q. Li, 2010: An interdecadal change in southern China summer rainfall around 1992–93. *J. Climate*, **23**, 2389–2403.
- Yang, H., S. Q. Sun, and J. Wei, 2006: The east-westward variation of summer western Pacific subtropical high and its influence to the climate. Wu, G. X., and Q. Zhang (eds.), *Advance in Research on Summer Subtropical High*. Meteorological Press, Beijing, 44–55 (in Chinese).
- Yao, C., S. Yang, W. Qian, Z. Lin, and M. Wen, 2008: Regional summer precipitation events on Asia and their changes in the past decades. *J. Geophys. Res.*, **113**, D17107, doi: 10.1029/2007JD009603.
- Yuan, Y., W. Zhou, J. C. L. Chan, and C. Y. Li, 2008a: Impacts of the basin-wide Indian Ocean SSTA on the South China Sea summer monsoon onset. *Int. J. Climatol.*, **28**, 1579–1587. DOI:10.1002/joc.1671.
- Yuan, Y., H. Yang, W. Zhou, and C. Y. Li, 2008b: Influences of the Indian Ocean Dipole on the Asian summer monsoon in the following year. *Int. J. Climatol.*, **28**, 1849–1859. DOI:10.1002/joc.167.
- Zhai, P. M., X. B. Zhang, H. Wan, and X. H. Pan, 2005: Trends in total precipitation and frequency of daily precipitation extremes over China. *J. Climate*, **18**, 1096–1108.
- Zhou, T. J., and R. C. Yu, 2005: Atmospheric water vapor transport associated with typical anomalous summer rainfall patterns in China. *J. Geophys. Res.*, **110**, D08104, doi: 10.1029/2004JD005413.
- Zhou, T. J., X. H. Zhang, and S. W. Wang, 1999: The air-sea freshwater exchange derived from NCEP/NCAR reanalysis data. *Acta Meteorol. Sinica*, **57**, 264–282 (in Chinese).
- Zhou, W., and J. C. L. Chan, 2005: Intraseasonal oscillations and the South China Sea summer monsoon onset. *Int. J. Climatol.*, **25**, 1585–1609.
- Zhou, W., J. C. L. Chan, and C. Y. Li, 2005: South China Sea summer monsoon onset in relation to the off-equatorial ITCZ. *Adv. Atmos. Sci.*, **22**, 665–676.
- Zhou, W., C. Y. Li, and J. C. L. Chan, 2006: The interdecadal variations of the summer monsoon rainfall over South China. *Meteor. Atmos. Phys.*, **96**, 165–175, DOI 10.1007/S00703-006-018-9.
- Zhou, W., J. C. L. Chan, W. Chen, J. Ling, J. G. Pinto, and Y. Shao, 2009: Synoptic-scale controls of persistent low temperature and icy weather over Southern china in January 2008. *Mon. Wea. Rev.*, **137**, 3978–3991, doi:10.1175/2009MWR2952.1.